# Effect of Tumor Perfusion and Receptor Density on Tumor Control Probability in $^{177}$Lu-DOTATATE Therapy: An In Silico Analysis for Standard and Optimized Treatment

Luis David Jiménez-Franco[1], Gerhard Glatting[2,3], Vikas Prasad[2], Wolfgang A. Weber[4], Ambros J. Beer[2], and Peter Kletting[2,3]

[1]*ABX-CRO Advanced Pharmaceutical Services Forschungsgesellschaft mbH, Dresden, Germany;* [2]*Department of Nuclear Medicine, Ulm University, Ulm, Germany;* [3]*Medical Radiation Physics, Department of Nuclear Medicine, Ulm University, Ulm, Germany; and* [4]*Department of Nuclear Medicine, Klinikum Rechts der Isar, Technische Universität München, Munich, Germany*

The aim of this work was to determine a minimal tumor perfusion and receptor density for $^{177}$Lu-DOTATATE therapy using physiologically based pharmacokinetic (PBPK) modeling considering, first, a desired tumor control probability (TCP) of 99% and, second, a maximal tolerated biologically effective dose ($BED_{max}$) for organs at risk (OARs) in the treatment of neuroendocrine tumors and meningioma. **Methods:** A recently developed PBPK model was used. Nine virtual patients (i.e., individualized PBPK models) were used to perform simulations of pharmacokinetics for different combinations of perfusion (0.001–0.1 mL/g/min) and receptor density (1–100 nmol/L). The TCP for each combination was determined for 3 different treatment strategies: a standard treatment (4 cycles of 7.4 GBq and 105 nmol), a treatment maximizing the number of cycles based on $BED_{max}$ for red marrow and kidneys, and a treatment having 4 cycles with optimized ligand amount and activity. The red marrow and the kidneys ($BED_{max}$ of 2 $Gy_{15}$ and 40 $Gy_{2.5}$, respectively) were assumed to be OARs. Additionally, the influence of varying glomerular filtration rates, kidney somatostatin receptor densities, tumor volumes, and release rates was investigated. **Results:** To achieve a TCP of at least 99% in the standard treatment, a minimal tumor perfusion of 0.036 ± 0.023 mL/g/min and receptor density of 34 ± 20 nmol/L were determined for the 9 virtual patients. With optimization of the number of cycles, the minimum values for perfusion and receptor density were considerably lower, at 0.022 ± 0.012 mL/g/min and 21 ± 11 nmol/L, respectively. However, even better results (perfusion, 0.018 ± 0.009 mL/g/min; receptor density, 18 ± 10 nmol/L) were obtained for strategy 3. The release rate of $^{177}$Lu (or labeled metabolites) from tumor cells had the strongest effect on the minimal perfusion and receptor density for standard and optimized treatments. **Conclusion:** PBPK modeling and simulations represent an elegant approach to individually determine the minimal tumor perfusion and minimal receptor density required to achieve an adequate TCP. This computational method can be used in the radiopharmaceutical development process for ligand and target selection for specific types of tumors. In addition, this method could be used to optimize clinical trials.

**Key Words:** minimal tumor perfusion; minimal receptor density; PBPK modeling; tumor control probability; $^{177}$Lu-DOTATATE

**J Nucl Med 2021; 62:92–98**
DOI: 10.2967/jnumed.120.245068

Tumor uptake of radioligands is determined by their affinity for their respective targets, the expression level of the target, and the perfusion. In molecular radiotherapy, perfusion can become a limiting factor for tumor uptake and absorbed dose when using ligands with a small molecular size that are rapidly cleared from the circulation by the kidneys (*1,2*). Because of the recent clinical success of molecular radiotherapy for neuroendocrine tumors (NETs) and prostate cancer, there is an enormous interest in identifying novel targets and radioligands to expand the use of molecular radiotherapy to other malignancies (*3,4*). Promising targets and ligands for further testing are currently selected by qualitative (semiquantitative) assessment of the target expression as well as by in vitro studies of the ligand affinity. In vivo tumor uptake is then usually assessed in tumor-bearing mice. However, these animal studies may be misleading because of marked differences between mouse and human cardiovascular physiology resulting in different blood clearance rates, as well as differences in perfusion between human tumors and subcutaneous xenografts (*5*). In addition, target expression may differ significantly between xenografts and human tumors. Therefore, a quantitative model to predict radioligand uptake in tumors on the basis of target expression levels and perfusion would be of great value for radioligand development and for optimization of the assessment process. Such a model could, for example, estimate the minimal tumor perfusion and target expression levels required to achieve a certain tumor control probability (TCP) while considering the maximum tolerated biologically effective doses ($BED_{max}$) for normal tissues.

To our knowledge, no systematic, quantitative analysis of the impact of receptor density and perfusion on tumor uptake of radioligands has been conducted. Furthermore, it has not been analyzed to what extent low tumor BED due to poor perfusion can be overcome by individualized treatment, such as by adjusting the injected activity and ligand amount or the number of treatment cycles (*6,7*). Whole-body physiologically based pharmacokinetic (PBPK) modeling allows addressing these questions (*8–11*). With known ranges of perfusion and

Received Mar. 13, 2020; revision accepted May 30, 2020.
For correspondence or reprints contact: Peter Kletting, Department of Nuclear Medicine, Ulm University, D-89081 Ulm, Germany.
E-mail: peter.kletting@uniklinik-ulm.de
Published online Jul. 9, 2020.

**TABLE 1**
Investigated Treatment Strategies as Determined by Number of Cycles, Used Ligand Amount, Activity, and OAR Boundary Conditions

| Strategy | Number of cycles | Ligand amount | Activity | Boundary condition |
|---|---|---|---|---|
| 1 | 4 | 105 nmol | 7.4 GBq | None* |
| 2 | Maximized† | 105 nmol | 7.4 GBq | Kidney $BED_{max} \leq 40\ Gy_{2.5}$ and red marrow $BED_{max} \leq 2\ Gy_{15}$ |
| 3 | 4 | Optimal‡ | Optimal‡ | Kidney $BED_{max} \leq 40\ Gy_{2.5}$ and red marrow $BED_{max} \leq 2\ Gy_{15}$ |

*Not reached for all patients.
†Maximized considering OAR $BED_{max}$.
‡Maximal activity to be administered is calculated for amounts of 25, 50, 75, 100, 125, 150, 175, 200, 250, 350, and 500 nmol. Combination of amount and maximal activity resulting in highest TCP is selected.

receptor density in tumor and other physiologic parameters for normal tissues, simulations can determine the feasibility of using that target structure for therapy and optimize the administered ligand amount and activity.

In this study, we performed such an analysis for the treatment of NETs and meningioma with $^{177}$Lu-DOTATATE, a peptide with high affinity for the somatostatin receptor type 2 (SSTR2) (*6,7*). Specifically, we determined the minimal tumor perfusion and receptor density based on PBPK modeling considering a desired TCP of 99% and the $BED_{max}$ for organs at risk (OARs). The TCP was calculated for various combinations of tumor perfusion (0.001–0.1 mL/g/min) and receptor density (1–100 nmol/L) in 9 virtual patients (i.e., individualized PBPK models) with NETs ($n = 5$) or meningioma ($n = 4$). Kidneys ($BED_{max}$, 40 $Gy_{2.5}$) and red marrow ($BED_{max}$, 2 $Gy_{15}$) were considered to be OARs. One tumor lesion per virtual patient was investigated. The TCP was calculated for each virtual patient and each combination of tumor perfusion and receptor density for standard and optimized therapy. Additionally, we determined the influence of the glomerular filtration rate (GFR), kidney SSTR2 density, release rate of $^{177}$Lu/radiolabeled metabolites from tumor cells, and tumor volume.

## MATERIALS AND METHODS

### PBPK Model

The development of the PBPK model and the estimation of the individual model parameters for the virtual patients are described elsewhere (*6,7*) and in the supplemental material (Supplemental File A [supplemental materials are available at http://jnm.snmjournals.org]; Tables 1–3). In brief, all major physiologic and physical mechanisms, that is, distribution via blood flow, binding to serum proteins, extravasation, nonlinear SSTR2-specific binding, internalization, degradation and release, excretion, and physical decay, are included in the model (Supplemental File A; Figs. 1–3). Kidney uptake is assumed to be predominantly SSTR2-specific because of the high kidney SSTR2 expression, the high affinity of $^{177}$Lu-DOTATATE to the SSTR2, and the administration of amino acids, which substantially decreases the nonspecific uptake. One tumor lesion per virtual patient was considered. The model was implemented in Matlab/Simulink, version R2017a (MathWorks).

**TABLE 2**
Individual Minimal Tumor Perfusion and Receptor Density for Each Virtual Patient and Evaluated Strategy to Achieve TCP > 99%

| | Strategy 1 | | Strategy 2 | | Strategy 3 | | Actual value | |
|---|---|---|---|---|---|---|---|---|
| Virtual patient | $f_{tu,min}$ (mL/g/min) | $[R]_{tu,min}$ (nmoL/L) | $f_{tu,min}$ (mL/g/min) | $[R]_{tu,min}$ (nmol/L) | $f_{tu,min}$ (mL/g/min) | $[R]_{tu,min}$ (nmol/L) | $f_{tu}$ (mL/g/min) | $[R]_{tu}$ (nmol/L) |
| 1 | 0.044 | 41 | 0.025 | 23 | 0.019 | 19 | 0.1 | 15 |
| 2 | 0.051 | 47 | 0.028 | 27 | 0.023 | 22 | 0.1 | 24 |
| 3 | 0.054 | 53 | 0.036 | 35 | 0.029 | 31 | 0.9 | 5 |
| 4 | 0.072 | 63 | 0.031 | 27 | 0.026 | 25 | 1.0 | 30 |
| 5 | 0.004 | 5 | 0.004 | 5 | 0.004 | 4 | 0.1 | 29 |
| 6 | 0.043 | 42 | 0.024 | 24 | 0.021 | 21 | 1.0 | 19 |
| 7 | 0.011 | 10 | 0.006 | 6 | 0.006 | 5 | 0.03 | 11 |
| 8 | 0.011 | 15 | 0.011 | 15 | 0.011 | 10 | 0.02 | 16 |
| 9 | 0.032 | 31 | 0.032 | 31 | 0.022 | 29 | 0.06 | 14 |
| Mean | 0.036 | 34.1 | 0.022 | 21.4 | 0.018 | 18.4 | 0.4 | 18 |
| SD | 0.023 | 20.2 | 0.012 | 10.6 | 0.009 | 10.0 | 0.4 | 8 |
| Median | 0.044 | 42 | 0.025 | 24 | 0.021 | 21 | 0.1 | 16 |
| Minimum | 0.004 | 5 | 0.004 | 5 | 0.004 | 4 | 0.02 | 5 |
| Maximum | 0.072 | 63 | 0.036 | 35 | 0.029 | 31 | 1.0 | 30 |

$f_{tu,min}$ = minimal tumor perfusion; $[R]_{tu,min}$ = minimal tumor receptor density; $f_{tu}$ = fitted tumor perfusion; $[R]_{tu}$ = fitted tumor receptor density.

**TABLE 3**
Influence of Varying Tumor and Normal-Tissue Parameters on Minimal Tumor Perfusion and Receptor Density in Population-Median Virtual Patient

| Parameter | Parameter value | Strategy 1 | | Strategy 2 | | Strategy 3 | |
|---|---|---|---|---|---|---|---|
| | | $f_{tu,min}$ (mL/g/min) | $[R]_{tu,min}$ (nmol/L) | $f_{tu,min}$ (mL/g/min) | $[R]_{tu,min}$ (nmol/L) | $f_{tu,min}$ (mL/g/min) | $[R]_{tu,min}$ (nmol/L) |
| Release rate ($min^{-1}$) | $10^{-3}$ | 0.100* | 100* | 0.065 | 62 | 0.055 | 54 |
| | $10^{-4}$ | 0.032 | 31 | 0.018 | 18 | 0.016 | 16 |
| | $10^{-5}$ | 0.017 | 16 | 0.010 | 9 | 0.009 | 8 |
| | $10^{-6}$ | 0.015 | 15 | 0.009 | 8 | 0.008 | 7 |
| Tumor volume (mL) | 0.1 | 0.035 | 35 | 0.020 | 20 | 0.018 | 17 |
| | 1 | 0.041 | 41 | 0.024 | 23 | 0.021 | 20 |
| | 10 | 0.047 | 47 | 0.027 | 26 | 0.024 | 23 |
| | 100 | 0.049 | 49 | 0.028 | 27 | 0.024 | 24 |
| GFR (mL/min) | 30 | 0.023 | 24 | 0.029 | 33 | 0.021 | 28 |
| | 60 | 0.036 | 36 | 0.029 | 29 | 0.024 | 24 |
| | 90 | 0.048 | 48 | 0.027 | 27 | 0.024 | 23 |
| | 120 | 0.06 | 59 | 0.026 | 26 | 0.024 | 23 |
| Kidney receptor density (nmol/L) | 2.5 | 0.047 | 46 | 0.017 | 16 | 0.018 | 15 |
| | 5 | 0.047 | 47 | 0.021 | 20 | 0.021 | 20 |
| | 7.5 | 0.048 | 48 | 0.032 | 31 | 0.025 | 25 |
| | 10 | 0.049 | 48 | 0.049 | 48 | 0.027 | 33 |

*Did not reach 99% TCP within simulated ranges for tumor perfusion and receptor density.
$f_{tu,min}$ = minimal tumor perfusion; $[R]_{tu,min}$ = minimal tumor receptor density.

### Virtual Patients

In this work, a virtual patient is defined as a PBPK model with a set of parameters determined by fitting the model to individual time–activity data and directly measured quantities. The model and individual model parameters were taken from Jiménez-Franco et al. (*7*). We investigated 9 virtual patients that differed in GFR, SSTR2 expression in normal tissue, tumor volume, release rates from tumor and normal tissue, and other individualized parameters (Supplemental File A; Tables 2 and 3). No changes in tumor perfusion or receptor expression between the cycles were assumed, and no tumor growth or shrinkage was considered.

### Absorbed Dose, Biologically Effective Dose, and TCP

The PBPK model structure was combined with a radiobiologic model for BED and TCP calculations (Supplemental File B). Absorbed doses, BEDs, and TCPs were calculated as described by Jiménez-Franco et al. (Supplemental File B) (*7*). In short, absorbed doses considering only self-irradiation were calculated for the kidneys, whereas for the red marrow both self- and cross-irradiation were considered (Supplemental File B; Table 1). Tumor absorbed doses were calculated using a sphere model (Supplemental File B; Table 2) (*12*).

For the BED calculations, α/β ratios (the parameters of the linear-quadratic model of cell survival) of 2.5, 15, and 10 Gy were assumed for the kidneys, red marrow, and tumor lesions, respectively (Supplemental File B) (*7*). The cell repair rates used for the BED calculations were ln(2)/2.8 $h^{-1}$ for the kidneys, ln(2)/1.0 $h^{-1}$ for the red marrow, and ln(2)/1.5 $h^{-1}$ for the tumor lesions (*13*).

TCPs were determined assuming that the cell survival fraction was equal for all cycles and that there were no physiologic or radiobiologic changes in the organ or tumor parameters throughout the cycles. Thus, Equation 1 was used for the TCP calculations for multiple cycles as follows (Supplemental File B) (*7*):

$$\mathrm{TCP} = e^{-n_0 \cdot \left(SF_c^{Nc}\right)}, \qquad \text{Eq. 1}$$

where $n_0$ is the initial number of tumor clonogenic cells, $SF_c$ is the tumor survival fraction for the first dose cycle, and $Nc$ is the number of cycles. The number of clonogenic cells for each lesion was determined considering its mass and a clonogenic cell density of $1.12 \times 10^5$ cells/g (*14*). Survival fractions were calculated from the BEDs assuming a radiosensitivity value α of 0.35 $Gy^{-1}$ for all tumor lesions (*14*).

### Simulations with Individual Virtual Patients

The TCPs were calculated for different combinations of tumor receptor density (i.e., number of receptors per mass, $[R]_{tu}$) and perfusion (i.e., blood flow per mass, $f_{tu}$). All other parameters of the virtual patients were unchanged. The tumor perfusion and receptor density were varied from 0.001 to 0.1 mL/g/min (steps of 0.001 mL/g/min) and from 1 to 100 nmol/L (steps of 1 nmol/L), respectively. The choices for the maximal investigated tumor receptor densities and perfusion values were based on the literature (*6,15*).

### Different Treatment Strategies

The TCP was investigated for all combinations of tumor receptor density and perfusion for standard $^{177}$Lu-DOTATATE therapy (4 cycles of 7.4 GBq and 105 nmol) (strategy 1) (*16*) and for individualized therapy based on dosimetry results (strategy 2) and on the estimated optimal ligand amount and activity (strategy 3) (Table 1). For strategies 1 and 2, a ligand amount of 105 nmol (~150 μg) is used to represent the standard therapy, as the consensual ligand amount is between 100 μg (~70 nmol) and 200 μg (~139 nmol) (*16*). For strategies 2 and 3, the

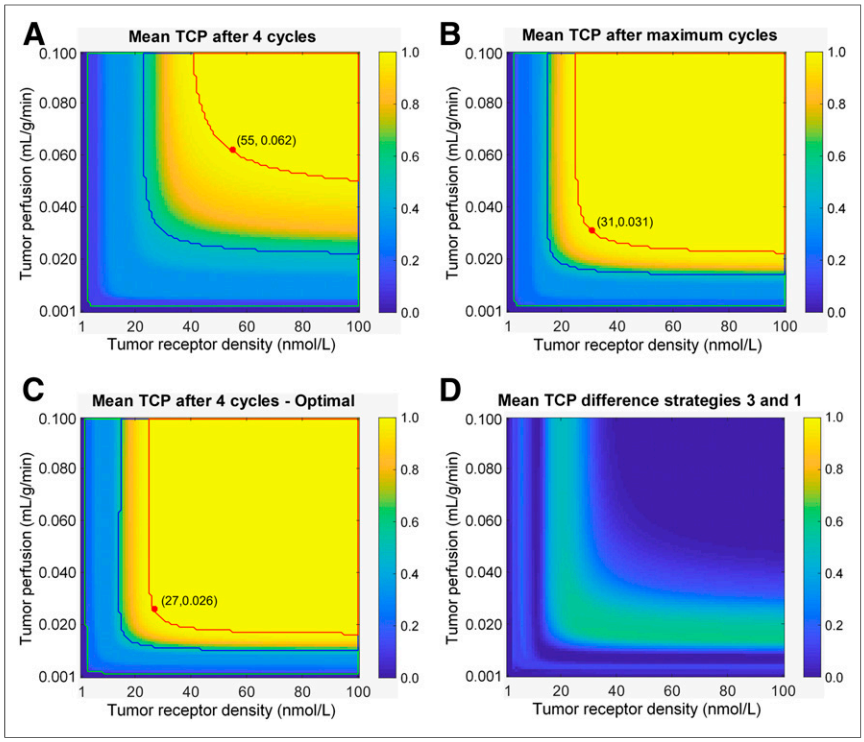


**FIGURE 1.** Mean TCP of all virtual patients is shown for different combinations of tumor perfusion and receptor density for different therapy strategies. (A) Simulation of standard treatment (strategy 1). (B) Optimization of number of cycles (strategy 2). (C) Optimization of ligand amount and activity (strategy 3). Green, blue, and red iso-TCP lines represent TCPs of 1%, 50%, and 99%, respectively. Red stars show combination of tumor perfusion and receptor density yielding TCP ≥ 99% with smallest standardized Euclidean distance to origin (0 nmol/L, 0 mL/g/min). (D) Mean TCP difference between strategy 3 and strategy 1.

kidneys and the red marrow were assumed to be the OARs, with a $BED_{max}$ of 40 $Gy_{2.5}$ and 2 $Gy_{15}$, respectively (*7*). For strategy 3, the highest TCP without exceeding $BED_{max}$ for the kidneys and the red marrow (*7*) was determined by simulations with different ligand amounts (25, 50, 75, 100, 125, 150, 175, 200, 250, 350, and 500 nmol) and pertaining maximal activities (*7*).

Additionally, the actual dose-limiting organ (kidneys or red marrow) was identified for each combination of tumor perfusion and receptor density for all virtual patients.

### Simulations with Population-Median Virtual Patient

To analyze the influence of other important parameters on the minimal tumor receptor density and perfusion, simulations with 2 tumor-specific and 2 normal-tissue–specific parameters were conducted for all strategies for a population-median virtual patient with median parameters from the 9 virtual patients: The effects of varying the tumor volume (0.1, 1, 10, and 100 mL), the release rate from the tumor ($10^{-3}$, $10^{-4}$, $10^{-5}$, and $10^{-6}$ $min^{-1}$) (*17*), GFR (30, 60, 90, and 120 $mL \cdot min^{-1}$), and SSTR2 expression in the kidneys (2.5, 5, 7.5, and 10 $nmol \cdot mL^{-1}$) (*6,7*) were investigated. These parameters were selected because they vary considerably among the virtual patients, with tumor volume ranging from 2 to 2,520 mL, release rate from the tumor ranging from 0 to $3 \cdot 10^{-4}$ $min^{-1}$, GFR ranging from 28 to 133 mL/min, and SSTR2 density in the kidneys ranging from 2.3 to 8.8 nmol/L.

### Definition of Minimal Tumor Perfusion and Receptor Density

As there is no unique combination of tumor perfusion and receptor density leading to a TCP of at least 99%, and to ease the comparison for the different simulations, the combination with the smallest standardized Euclidean distance (standardized by range) to the origin (0 nmol/L, 0 mL/g/min) was selected to represent the minimum tumor perfusion and receptor density.

## RESULTS

### Minimal Tumor Perfusion and Receptor Density

Figure 1 shows the simulation results for all combinations of tumor perfusion and receptor density averaged over the virtual patients for the studied strategies. For a standard treatment schedule of $^{177}$Lu-DOTATATE, a minimum SSTR2 density of 55 nmol/L and a minimum perfusion of 0.062 mL/g/min are necessary for a TCP of at least 99% (Fig. 1A). For strategy 2, the minimum tumor perfusion and SSTR2 density are 0.031 mL/g/min and 31 nmol/L, respectively (Fig. 1B). For strategy 3, the minimum values are 0.026 mL/g/min and 27 nmol/L, respectively (Fig. 1C). For a receptor density of less than 25 nmol/L, a TCP of at least 99% could not be achieved for any of the evaluated perfusion values and strategies. The minimal tumor perfusion and receptor density were considerably lower, on average, for strategy 2 than for strategy 1 (Fig. 1B compared with 1A, respectively). A further improvement was observed for strategy 3 (Fig. 1D). Table 2 presents one combination (defined by the smallest standardized Euclidian distance) of the minimal tumor perfusion and receptor density for each strategy and each virtual patient to achieve a TCP of at least 99%.

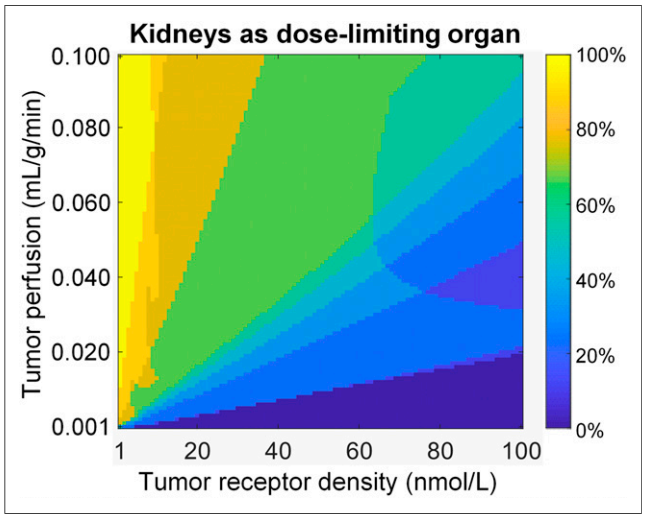


**FIGURE 2.** Fraction of virtual patients for which kidneys are dose-limiting with strategy 3 for each combination of tumor perfusion and receptor density; 100% reflects that for these combinations, kidneys were dose-limiting in all patients.

### Dose-Limiting Organs

The defined BED limits for the OARs were not exceeded for any of the 9 virtual patients with strategy 1. For strategy 2, the $BED_{max}$

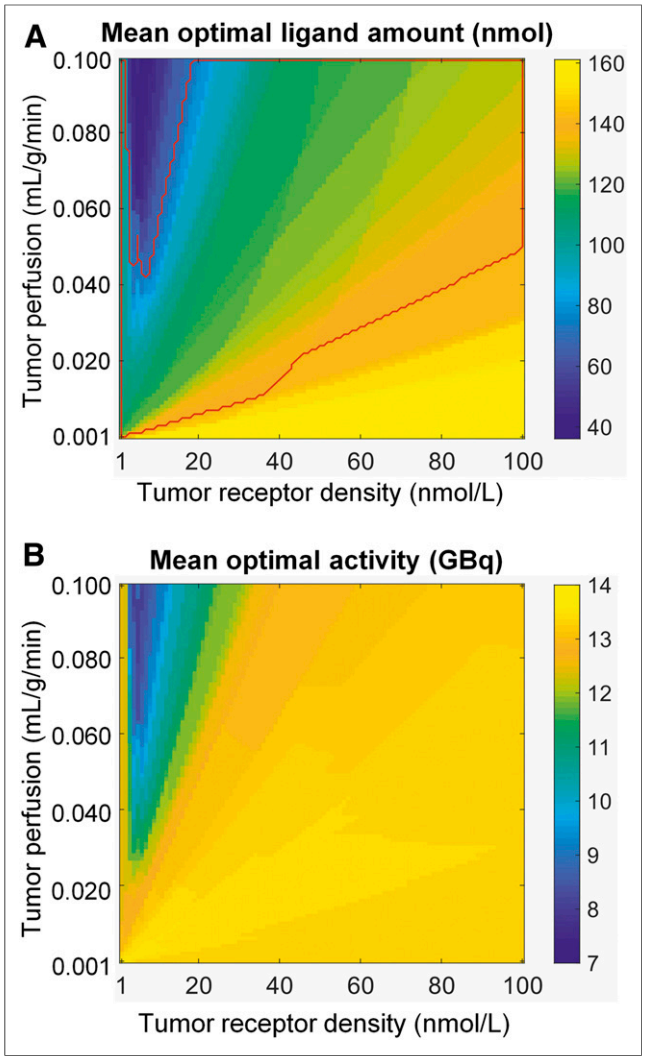


**FIGURE 3.** Mean optimal amounts (A) and activities (B) for 1 cycle for each combination of tumor perfusion and receptor density, applying strategy 3. Red line contours mean optimal amounts between 70 nmol (~100 μg) and 139 nmol (~200 μg), which is the consensual range of ligand amounts suggested by the European Association of Nuclear Medicine guidelines for therapy with peptides labeled with $^{177}$Lu (*16*). Mean optimal activity was higher than the suggested maximum activity (7.4 GBq) for $^{177}$Lu-DOTATATE treatment by the European Association of Nuclear Medicine guidelines for all explored combinations (*16*).

for the kidneys ($n = 6$) or red marrow ($n = 3$) was reached after 4–9 cycles (median, 6). Figure 2 shows the fraction among all virtual patients in which the kidneys were the dose-limiting organ for strategy 3. For the remaining virtual patients, the red marrow was dose-limiting (Fig. 2 subtracted from 100%). For strategy 3, the likelihood that the kidneys are the dose-limiting organ increases with increasing tumor perfusion and decreasing receptor density (Fig. 2) because lower ligand amounts are required for optimal TCP (Fig. 3A). On the other hand, for strategy 3, the higher the receptor density and the lower the perfusion, the more likely is the red marrow to be dose-limiting (Fig. 2) because of increasing optimal ligand amounts (Fig. 3A).

### Optimal Amounts and Activities

Figure 3 depicts the optimal peptide amount (Fig. 3A) and activity (Fig. 3B) for all combinations averaged over all virtual patients. A red line encompassing the consensual peptide amount range (70–139 nmol) is shown in Figure 3A (*16*). The average optimal activity was higher than the suggested maximum activity (7.4 GBq) for all explored combinations (Fig. 3B) (*16*). Figure 3A shows that for higher perfusion (>0.059 mL/g/min) and lower receptor density (<11 nmol/L), the optimal peptide amount is lower than the minimal consensual ligand amount (70 nmol). Similarly, for low tumor perfusion (<0.027 mL/g/min) and high receptor density (>60 nmol/L), the optimal amount is higher than the maximal consensual ligand amount (139 nmol). However, the optimal amounts are within the consensus range for most of the investigated combinations of tumor perfusion and receptor density.

### Simulations with Population-Median Virtual Patient

The results for the simulations with the population-median virtual patient are presented in Table 3. The tumor release rate is the most sensitive parameter in all strategies. The effect of changes in GFR is stronger for strategy 1, where for higher GFRs, higher tumor perfusions and receptor densities are required to achieve a TCP of at least 99%. The influence of variations in GFR is considerably reduced by optimizing cycles or ligand amount and activity. Variations in tumor volume produce a relatively small variation in minimum tumor perfusion and receptor density for all evaluated strategies (Table 3).

## DISCUSSION

PBPK modeling is increasingly used in developing drugs and optimizing therapy (*18*). Here, we used a mathematic model combining a PBPK structure with BED and TCP calculations (*6,7*) to investigate the effect of tumor perfusion and SSTR2 receptor density on the effectiveness of $^{177}$Lu-DOTATATE therapy in patients with NETs and meningioma.

Our results indicate that for a standard treatment, a minimum SSTR2 density of 55 nmol/L and a minimum perfusion of 0.062 mL/g/min are necessary for a TCP of at least 99% (Fig. 1A). As this combination is presented for the standardized Euclidian distance to the origin, receptor densities of more than 55 nmol/L may allow for a TCP of at least 99%, even at lower tumor perfusions (Fig. 1). Conversely, higher perfusions could to some extent compensate for a lower receptor density. Nevertheless, our simulations indicate that well-defined limits exist for both tumor receptor density and perfusion that determine the effectiveness of the $^{177}$Lu-DOTATATE therapy.

A second important finding of our study is that individualized treatment strategies considering $BED_{max}$ for the red marrow and the kidneys can substantially reduce the limitations for tumor perfusion and receptor density (Figs. 1B–1D). By adjusting the peptide amount and injected activity, a TCP of at least 99% was achieved for a 2-fold lower receptor density and a 2.4-fold lower tumor perfusion than with standard treatment (Fig. 1).

These findings have several implications for $^{177}$Lu-DOTATATE therapy. First, the findings ensure that for standard and optimized $^{177}$Lu-DOTATATE therapy, the calculated individual minimal perfusions (~0.004–0.07 mL/g/min) are well below the average tumor perfusions of NET primaries (*19*), NET metastases (*20*), or meningiomas (*21*) (all >0.1 mL/g/min). Thus, tumor perfusion does not appear to be a limiting factor for $^{177}$Lu-DOTATATE therapy for these diseases. However, the tumor SSTR2 expression found in these virtual patients (determined by fitting to time–activity data in Kletting et al. (*6*)) is about 1.9-fold lower on average than the herein-identified minimal receptor density for standard

therapy, 1.2-fold lower for optimized cycles, and similar for optimized ligand amount and activity (Table 2). Thus, effectiveness can potentially be improved by ligands with higher SSTR2 density or longer tumor retention such as some SSTR2 antagonists that have recently entered clinical testing (*22*).

Second, our results strongly argue for performing dosimetry to improve the success of $^{177}$Lu-DOTATATE therapy. Peritherapeutic measurements and absorbed dose calculations help in deciding whether to increase the number of cycles compared with the standard treatment (median optimal number of cycles, 6). A further improvement would be treatment planning in which ligand amount and activity are individualized before the first cycle. Incorporating PET/MRI or PET/CT measurements in combination with additional prior knowledge (e.g., GFR measurements) and PBPK modeling might allow individual estimation of perfusion and receptor density in the clinically most relevant lesions before therapy. Thus, tailoring therapy might substantially increase the TCP for many NETs and meningiomas. However, to fully incorporate such approaches into clinical decision making, these models need to be refined regarding tumor changes after each cycle (*8*).

The application of this PBPK model goes beyond optimizing $^{177}$Lu-DOTATATE treatment of NETs and meningioma, as SSTR2 is expressed by a variety of other malignancies such as non-Hodgkin lymphoma and renal cell cancer (*3,4*). Thus, PBPK modeling can be used to assess whether molecular radiotherapy with $^{177}$Lu-DOTATATE or with other SSTR2 ligands is potentially effective for these tumor types or whether the perfusion or the SSTR2 expression is too low to achieve the expected therapeutic effect. Furthermore, PBPK modeling and the proposed method can also be applied for novel targets as soon as the typical ranges for the number of binding sites and for the perfusion of the targeted tumor type are known.

In general, the complexity of PBPK models (*23*) depends on knowledge of the biologic systems and the scientific question to be answered. To demonstrate the relationship among perfusion, receptor density, activity, and ligand amount, in scenario 3 we optimized the TCP for only 1 tumor lesion. Consequently, the intraindividual variability of the tumor characteristics was not considered—a factor that could have influenced the TCP calculations. For treatment planning, more lesions could be considered, as described by Jiménez-Franco et al. (*7*). For the actual treatment planning, including temporal and spatial changes in tumor SSTR2 expression, perfusion, and radiosensitivity might improve the predictions. Heterogeneity in target expression, perfusion, and radiosensitivities at the microscopic level may lead to an inhomogeneous absorbed dose distribution. It is currently unknown how this heterogeneity will affect the TCP in molecular radiotherapy, and the effect may vary for different radionuclides. However, in principle, this heterogeneity could be included in the model once data on the microscopic heterogeneity of the SSTR2 expression, perfusion, and radiosensitivity become available.

## CONCLUSION

A method based on PBPK and radiobiologic modeling was developed to identify a minimal tumor perfusion and receptor density that allows a defined (here $\geq$ 99%) TCP after $^{177}$Lu-DOTATATE therapy. The algorithm takes into account previously determined expression levels in normal tissues and BED limits for the kidneys and the red marrow. The method can easily be adapted to other tumors or ligands and might be helpful in the development and validation of new ligands and in the optimization of clinical trials.

## DISCLOSURE

This work was supported by grants KL2742/2-1, BE4393/1-1, GL236/11-1, SFB824 (project B11), and SFB1279 (project Z02) from the Deutsche Forschungsgemeinschaft (German Research Foundation). No other potential conflict of interest relevant to this article was reported.

## KEY POINTS

**QUESTION:** What is the minimal tumor perfusion and receptor density for a successful treatment using a specific target (here SSTR2) and ligand in $^{177}$Lu-DOTATATE therapy?

**PERTINENT FINDINGS:** The minimal flow and receptor density for achieving a TCP of at least 99% for a standard therapy were 0.036 ± 0.023 mL/g/min and 34 ± 20 nmol/L. These parameter values were determined for 9 virtual patients using PBPK and radiobiologic modeling. Individually optimizing the number of cycles or the ligand and activity amount allows even considerably lower perfusion and receptor densities.

**IMPLICATIONS FOR PATIENT CARE:** Individually optimized therapy with $^{177}$Lu-DOTATATE with respect to the number of cycles or the amounts of ligand and activity may considerably improve therapy.

## REFERENCES

1. Thurber GM, Weissleder R. A systems approach for tumor pharmacokinetics. *PLoS One.* 2011;6:e24696.
2. Thurber GM, Weissleder R. Quantitating antibody uptake in vivo: conditional dependence on antigen expression levels. *Mol Imaging Biol.* 2011;13:623–632.
3. Haberkorn U, Mier W, Kopka K, Herold-Mende C, Altmann A, Babich J. Identification of ligands and translation to clinical applications. *J Nucl Med.* 2017; 58(suppl):27S–33S.
4. Reubi JC, Waser B, Mäcke H, Rivier J. Highly increased $^{125}$I-JR11 antagonist binding in vitro reveals novel indications for sst2 targeting in human cancers. *J Nucl Med.* 2017;58:300–306.
5. White CR, Kearney MR. Metabolic scaling in animals: methods, empirical results, and theoretical explanations. *Compr Physiol.* 2014;4:231–256.
6. Kletting P, Kull T, Maaß C, et al. Optimized peptide amount and activity for $^{90}$Y-labeled DOTATATE therapy. *J Nucl Med.* 2016;57:503–508.
7. Jiménez-Franco LD, Kletting P, Beer AJ, Glatting G. Treatment planning algorithm for peptide receptor radionuclide therapy considering multiple tumor lesions and organs at risk. *Med Phys.* 2018;45:3516–3523.
8. Kletting P, Thieme A, Eberhardt N, et al. Modeling and predicting tumor response in radioligand therapy. *J Nucl Med.* 2019;60:65–70.
9. Begum NJ, Thieme A, Eberhardt N, et al. The effect of total tumor volume on the biologically effective dose of tumor and kidneys for $^{177}$Lu-labelled PSMA peptides. *J Nucl Med.* 2018;59:929–933.
10. Kletting P, Schuchardt C, Kulkarni HR, et al. Investigating the effect of ligand amount and injected therapeutic activity: a simulation study for $^{177}$Lu-labeled PSMA-targeting peptides. *PLoS One.* 2016;11:e0162303.
11. Thiel C, Smit I, Baier V, et al. Using quantitative systems pharmacology to evaluate the drug efficacy of COX-2 and 5-LOX inhibitors in therapeutic situations. *NPJ Syst Biol Appl.* 2018;4:28.
12. Stabin MG, Siegel JA. Physical models and dose factors for use in internal dose assessment. *Health Phys.* 2003;85:294–310.
13. Cremonesi M, Botta F, Di Dia A, et al. Dosimetry for treatment with radiolabelled somatostatin analogues: a review. *Q J Nucl Med Mol Imaging.* 2010; 54:37–51.
14. Fowler JF. 21 years of biologically effective dose. *Br J Radiol.* 2010;83:554–568.
15. Vaupel P, Kallinowski F, Okunieff P. Blood flow, oxygen and nutrient supply, and metabolic microenvironment of human tumors: a review. *Cancer Res.* 1989;49: 6449–6465.

16. Bodei L, Mueller-Brand J, Baum RP, et al. The joint IAEA, EANM, and SNMMI practical guidance on peptide receptor radionuclide therapy (PRRNT) in neuroendocrine tumours. *Eur J Nucl Med Mol Imaging.* 2013;40: 800–816.
17. Fung EK, Cheal SM, Fareedy SB, et al. Targeting of radiolabeled J591 antibody to PSMA-expressing tumors: optimization of imaging and therapy based on non-linear compartmental modeling. *EJNMMI Res.* 2016;6:7.
18. Wagner C, Zhao P, Pan Y, et al. Application of physiologically based pharmacokinetic (PBPK) modeling to support dose selection: report of an FDA public workshop on PBPK. *CPT Pharmacometrics Syst Pharmacol.* 2015;4: 226–230.
19. Yao JC, Phan AT, Hess K, et al. Perfusion computed tomography as functional biomarker in randomized run-in study of bevacizumab and everolimus in well-differentiated neuroendocrine tumors. *Pancreas.* 2015;44:190–197.
20. Guyennon A, Mihaila M, Palma J, Lombard-Bohas C, Chayvialle JA, Pilleul F. Perfusion characterization of liver metastases from endocrine tumors: computed tomography perfusion. *World J Radiol.* 2010;2:449–454.
21. Kimura H, Takeuchi H, Koshimoto Y, et al. Perfusion imaging of meningioma by using continuous arterial spin-labeling: comparison with dynamic susceptibility-weighted contrast-enhanced MR images and histopathologic features. *AJNR Am J Neuroradiol.* 2006;27:85–93.
22. Reidy-Lagunes D, Pandit-Taskar N, O'Donoghue JA, et al. Phase I trial of well-differentiated neuroendocrine tumors (NETs) with radiolabeled somatostatin antagonist $^{177}$Lu-satoreotide tetraxetan. *Clin Cancer Res.* 2019;25:6939–6947.
23. Begum NJ, Glatting G, Wester H-J, Eiber M, Beer AJ, Kletting P. The effect of ligand amount, affinity and internalization on PSMA-targeted imaging and therapy: a simulation study using a PBPK model. *Sci Rep.* 2019;9:20041.